Developing a flux model to explore the effects of MCP compartmentalization on fluxes and metabolite concentrations in the 1,3-PDO pathway

Joy Nyaanga – Winter Rotation 2019

Objective

Compartmentalization strategies are utilized by various organisms to address problems of toxicity, leakage and byproduct accumulation during metabolism. Bacteria, in particular, have subcellular protein-bound organelles called microcompartments that contain essential enzymes for particular metabolic pathways. Exploiting this natural tool with metabolic engineering will allow for efficient biosynthesis, particularly in systems requiring redox cofactor recycling. A systems level examination of the benefits of this unique spatial organization technique will provide an understanding for how microcompartments work to minimize toxic intermediates, sequester private cofactor pools, and enhance overall pathway flux. I will accomplish this through the development of a mathematical model for the function of a microcompartment in 1,3-propanediol production.

Specific Objective: Establish a kinetic metabolic model to explore the spatial effect of compartmentalization.

Background

Bacterial microcompartments (MCPs) allow for the spatial organization of metabolism and thus are essential for enhancing biochemical reactions. Most bacterial cells contain several of these small 150 nm sized structures containing enzymes necessary to carry out certain metabolic pathways [1]. Utilizing these structures in bioengineered bacterial systems can allow for high-yield production of biofuels. This is noteworthy as biofuel production requires redox cofactors, many of which are consumed in other cellular processes.

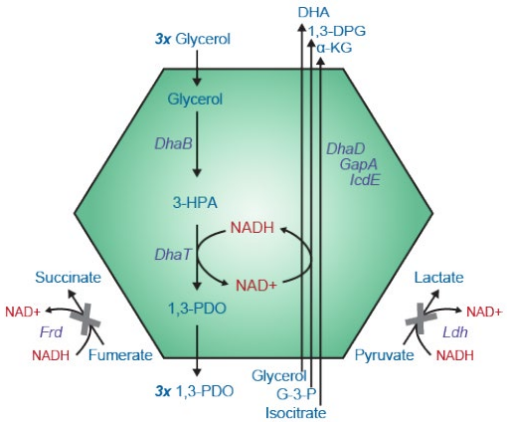

Figure 1.

The 1,3-propanediol (1,3-PDO) pathway is a great candidate for this form of metabolic engineering as the product is used as a building block in the production of many plastics. 1,3-PDO is currently produced from glycerol through chemical synthesis at a high cost due to low selectivity and production of toxic intermediates [2]. In this pathway, glycerol dehydratase (DhaB) and NADH-dependent 1,3-PDO dehydrogenase (DhaT) reduce glycerol to 1,3-PDO with 3-hydroxy-propionaldehyde (3-HPA) as an intermediate (Figure 1) [3]. Co-compartmentalizing this pathway for the bioconversion of glycerol to 1,3-PDO with enzymes to recycle NAD to NADH should improve the production process and prevent loss of these important redox cofactors.

Many of the mechanistic hypotheses regarding MCPs are a challenge to test experimentally as direct measurement of small molecule concentrations in bacterial MCPs remains difficult. Employing a modeling strategy, however, will allow for the effects of the MCP on fluxes and metabolite concentrations to be characterized. Such a model will not only help determine how the MCP impacts thermodynamics across the network, but will also identify when compartmentalization will be most advantageous.

Approach

Compartmentalization strategy:

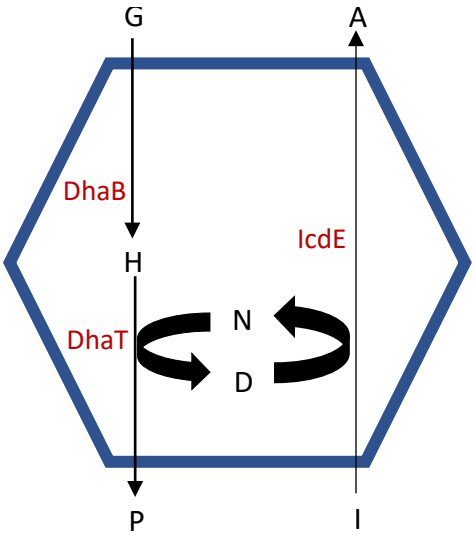

I have used a reaction-diffusion model incorporating passive transport across the MCP shell and the action of the DhaB, DhaT and IcdE enzymes within the MCP. The MCP is modeled as a spherical compartment of radius 100nm in solution (representing same fractional volume as five MCPs in a typical bacterial cell).

The following assumptions are also made:

1. I assume the MCP is spherically symmetrical
2. I consider constant external concentrations of glycerol, Isocitrate and 3-HPA
3. I assume the cofactors NAD+/NADH are unable to permeate the MCP membrane
4. I assume that the DhaB enzyme-catalyzed reactions are irreversible
5. I assume that the DhaT and IcdE enzyme-catalyzed reactions are reversible and have NAD+ or NADH cofactor sequential cofactor binding.
6. I assume solution inside and outside MCP is well mixed (diffusion is negligible).

The following equations for inside the MCP can be written:

$$\frac{dG}{dt} = -R_{DhaB}(G)$$

$$\frac{dH}{dt} = R_{DhaB}(G) - R_{DhaT}(H,N,P,D)$$

$$\frac{dP}{dt} = R_{DhaT}(H,N,P,D)$$

$$\frac{dI}{dt} = -R_{IcdE}(I,D,A,N)$$

$$\frac{dA}{dt} = R_{IcdE}(I,D,A,N)$$

$$\frac{dN}{dt} = -R_{DhaT}(H,N,P,D) + R_{IcdE}(I,D,A,N)$$

$$\frac{dD}{dt} = R_{DhaT}(H,N,P,D) - R_{IcdE}(I,D,A,N)$$

Inside the MCP, I assume Michaelis-Menten kinetic behavior of the DhaB, DhaT and IcdE enzymes, so the equation for the rate of the DhaB reaction is

$$R_{DhaB} = \frac{V_{DhaB} * G}{{K_M}^{DhaB} + G}$$

Here V_{DhaB} is the maximum rate of DhaB, and ${K_M}^{DhaB}$ is the half maximum concentration.

DhaT and IcdE are redox-coupled by the cycling of NAD+/NADH so I assume ordered bi-bi mechanism; the equations for the DHAT and IcdE reactions are therefore:

$$R_{DhaT} = \frac{\frac{{V_{f,DhaT}}^{max} * N * H}{{K_M}^{H} * {K_{I,DhaT}}^{N}} - \frac{{V_{r,DhaT}}^{max} * P * D}{{K_M}^{P} * {K_{I,DhaT}}^{D}}}{1 + \frac{N}{{K_{I,DhaT}}^{N}} + \frac{{K_{M,DhaT}}^{N} * H}{{K_{I,DhaT}}^{N} * {K_M}^{H}} + \frac{{K_{M,DhaT}}^{D} * P}{{K_M}^{P} * {K_{I,DhaT}}^{D}} + \frac{D}{{K_{I,DhaT}}^{D}} + \frac{N * H}{{K_{I,DhaT}}^{N} * {K_M}^{H}} + \frac{{K_{M,DhaT}}^{D} * N * P}{{K_{I,DhaT}}^{N} * {K_M}^{P} {K_{I,DhaT}}^{D}} + \frac{{K_{M,DhaT}}^{N} * H * D}{{K_{I,DhaT}}^{N} * {K_M}^{H} {K_{I,DhaT}}^{D}} + \frac{P * D}{{K_M}^{P} * {K_{I,DhaT}}^{D}} + \frac{N * H * P}{{K_{I,DhaT}}^{N} * {K_M}^{H} * {K_I}^{P}} + \frac{H * P * D}{{K_I}^{H} * {K_M}^{P} * {K_{I,DhaT}}^{D}}}$$

$$R_{IcdE} = \frac{\frac{{V_{f,IcdE}}^{max} * D * I}{{K_M}^{I} * {K_{I,IcdE}}^{D}} - \frac{{V_{r,IcdE}}^{max} * A * N}{{K_M}^{A} * {K_{I,IcdE}}^{N}}}{1 + \frac{D}{{K_{I,IcdE}}^{D}} + \frac{{K_{M,IcdE}}^{D} * I}{{K_{I,IcdE}}^{D} * {K_M}^{I}} + \frac{{K_{M,IcdE}}^{N} * A}{{K_M}^{A} * {K_{I,IcdE}}^{N}} + \frac{N}{{K_{I,IcdE}}^{N}} + \frac{D * I}{{K_{I,IcdE}}^{D} * {K_M}^{I}} + \frac{{K_{M,IcdE}}^{N} * D * A}{{K_{I,IcdE}}^{D} * {K_M}^{A} {K_{I,IcdE}}^{N}} + \frac{{K_{M,IcdE}}^{D} * I * N}{{K_{I,IcdE}}^{D} * {K_M}^{I} {K_{I,IcdE}}^{N}} + \frac{A * N}{{K_M}^{A} * {K_{I,DhaT}}^{N}} + \frac{D * I * A}{{K_{I,IcdE}}^{D} * {K_M}^{I} * {K_I}^{A}} + \frac{I * A * N}{{K_I}^{I} * {K_M}^{A} * {K_{I,DhaT}}^{N}}}$$

Here K_I's are inhibition constants.

I assume that G, H, P, I, and A are transported across the MCP membrane by passive diffusion, so I can specify the following boundary conditions to describe this continuity of flux

$$D\frac{\partial G(r)}{\partial r} = {k_c}^{G}(G(r)_{external} - G(r)_{MCP})$$

$$D\frac{\partial H(r)}{\partial r} = {k_c}^{H}(H(r)_{external} - H(r)_{MCP})$$

$$D\frac{\partial P(r)}{\partial r} = {k_c}^{P}(P(r)_{external} - P(r)_{MCP})$$

$$D\frac{\partial I(r)}{\partial r} = {k_c}^{I}(I(r)_{external} - I(r)_{MCP})$$

$$D\frac{\partial A(r)}{\partial r} = {k_c}^{A}(A(r)_{external} - A(r)_{MCP})$$

k_c: permeability of MCP to metabolites
$r = R_c$

I then derived nondimensional equations using the following scaling terms:

Variables:

$t = \tilde{t}\tau$

$G = \tilde{G} \cdot K_{M,DhaB}$

$H = \tilde{H} \cdot {K_M}^H$

$N = \tilde{N} \cdot {K_{M,DhaT}}^N$

$P = \tilde{P} \cdot {K_M}^P$

$D = \tilde{D} \cdot {K_{M,DhaT}}^D$

$I = \tilde{I} \cdot {K_M}^I$

$A = \tilde{A} \cdot {K_M}^A$

Parameters:

$$\alpha_1 = \frac{{K_{M,DhaT}}^N}{{K_{I,DhaT}}^N} \;;\; \alpha_2 = \frac{{K_{M,DhaT}}^D}{{K_{I,DhaT}}^D} \;;\; \alpha_3 = \frac{{K_M}^P}{{K_I}^P}$$

$$\alpha_4 = \frac{{K_M}^H}{{K_I}^H} \;;\; \alpha_5 = \frac{{V_{f,DhaT}}^{max}}{V_{DhaB}} \;;\; \alpha_6 = \frac{{V_{r,DhaT}}^{max}}{V_{DhaB}} \;;\; \xi = \frac{D \cdot K_{M,DhaB}}{V_{DhaB} \cdot {R_c}^2}$$

$$\beta_1 = \frac{{K_{M,DhaT}}^D}{{K_{I,IcdE}}^D} \;;\; \beta_2 = \frac{{K_{M,DhaT}}^N}{{K_{I,IcdE}}^N} \;;\; \beta_3 = \frac{{K_{M,IcdE}}^D}{{K_{I,IcdE}}^D} \;;\; \beta_4 = \frac{{K_{M,IcdE}}^N}{{K_{I,IcdE}}^N}$$

$$\beta_5 = \frac{{K_M}^A}{{K_I}^A} \;;\; \beta_6 = \frac{{K_M}^I}{{K_I}^I} \;;\; \beta_7 = \frac{{V_{f,IcdE}}^{max}}{V_{DhaB}} \;;\; \beta_8 = \frac{{V_{r,IcdE}}^{max}}{V_{DhaB}}$$

$$\varepsilon_1 = \frac{K_{M,DhaB}}{{K_{M,DhaT}}^H} \;;\; \varepsilon_2 = \frac{K_{M,DhaB}}{{K_{M,DhaT}}^P} \;;\; \varepsilon_3 = \frac{K_{M,DhaB}}{{K_{M,DhaT}}^N} \;;\; \varepsilon_4 = \frac{K_{M,DhaB}}{{K_{M,DhaT}}^D}$$

$$\varepsilon_5 = \frac{K_{M,DhaB}}{{K_{M,IcdE}}^A} \;;\; \varepsilon_6 = \frac{K_{M,DhaB}}{{K_{M,IcdE}}^I} \;;\; \tau = \frac{K_{M,DhaB}}{V_{DhaB}} \;;\; \chi = \frac{k_c \cdot K_{M,DhaB}}{V_{DhaB} \cdot R_c}$$

The equations to be integrated in time are as follows.

Inside the MCP:

$$\frac{d(\tilde{G})}{d\tilde{t}} = \frac{9(ngrid-{}^1/_2)^{4/3} * (G_{boundary}-G_{MCP})\cdot\xi}{(ngrid)^{1/3}} - \frac{\tilde{G}}{1+\tilde{G}} \tag{1.1}$$

$$\frac{d(\tilde{H})}{d\tilde{t}} = \frac{9(ngrid-{}^1/_2)^{4/3} * (H_{boundary}-H_{MCP})\cdot\xi}{(ngrid)^{1/3}} + \varepsilon_1 \left(\frac{\tilde{G}}{1+\tilde{G}} - \frac{\alpha_1\alpha_5\tilde{N}\tilde{H} + \alpha_2\alpha_6\tilde{P}\tilde{D}}{1+\alpha_1(\tilde{N}+\tilde{H}+\tilde{N}\tilde{H})+\alpha_2(\tilde{P}+\tilde{D}+\tilde{P}\tilde{D})+\alpha_1\alpha_2(\tilde{N}\tilde{P}+\tilde{H}\tilde{D})+\alpha_1\alpha_3(\tilde{H}\tilde{N}\tilde{P})+\alpha_2\alpha_4(\tilde{H}\tilde{P}\tilde{D})} \right) \tag{1.2}$$

$$\frac{d(\tilde{P})}{d\tilde{t}} = \frac{9(ngrid-{}^1/_2)^{4/3} * (P_{boundary}-P_{MCP})\cdot\xi}{(ngrid)^{1/3}} + \varepsilon_2 \left(\frac{\alpha_1\alpha_5\tilde{N}\tilde{H} - \alpha_2\alpha_6\tilde{P}\tilde{D}}{1+\alpha_1(\tilde{N}+\tilde{H}+\tilde{N}\tilde{H})+\alpha_2(\tilde{P}+\tilde{D}+\tilde{P}\tilde{D})+\alpha_1\alpha_2(\tilde{N}\tilde{P}+\tilde{H}\tilde{D})+\alpha_1\alpha_3(\tilde{H}\tilde{N}\tilde{P})+\alpha_2\alpha_4(\tilde{H}\tilde{P}\tilde{D})} \right) \tag{1.3}$$

$$\frac{d(\tilde{I})}{d\tilde{t}} = \frac{9(ngrid-{}^1/_2)^{4/3} * (I_{boundary}-I_{MCP})\cdot\xi}{(ngrid)^{1/3}} - \varepsilon_6 \left(\frac{\beta_1\beta_7\tilde{D}\tilde{I} - \beta_2\beta_8\tilde{A}\tilde{N}}{1+\beta_1(\tilde{D}+\tilde{D}\tilde{I})+\beta_3(\tilde{I})+\beta_2(\tilde{N}+\tilde{A}\tilde{N})+\beta_4(\tilde{A})+\beta_1\beta_4(\tilde{D}\tilde{A})+\beta_2\beta_3(\tilde{I}\tilde{N})+\beta_1\beta_5(\tilde{D}\tilde{I}\tilde{A})+\beta_2\beta_6(\tilde{I}\tilde{A}\tilde{N})} \right) \tag{1.4}$$

$$\frac{d(\tilde{A})}{d\tilde{t}} = \frac{9(ngrid-{}^{1}/_{2})^{4/3} * (A_{boundary}-A_{MCP})\cdot\xi}{(ngrid)^{1/3}} + \varepsilon_5 \left(\frac{\beta_1\beta_7\tilde{D}\tilde{I} - \beta_2\beta_8\tilde{A}\tilde{N}}{1+\beta_1(\tilde{D}+\tilde{D}\tilde{I})+\beta_3(\tilde{I})+\beta_2(\tilde{N}+\tilde{A}\tilde{N})+\beta_4(\tilde{A})+\beta_1\beta_4(\tilde{D}\tilde{A})+\beta_2\beta_3(\tilde{I}\tilde{N})+\beta_1\beta_5(\tilde{D}\tilde{I}\tilde{A})+\beta_2\beta_6(\tilde{I}\tilde{A}\tilde{N})} \right) \quad 1.5$$

$$\frac{d(\tilde{N})}{d\tilde{t}} = \varepsilon_3 \left(\frac{-\alpha_1\alpha_5\tilde{N}\tilde{H} + \alpha_2\alpha_6\tilde{P}\tilde{D}}{1+\alpha_1(\tilde{N}+\tilde{H}+\tilde{N}\tilde{H})+\alpha_2(\tilde{P}+\tilde{D}+\tilde{P}\tilde{D})+\alpha_1\alpha_2(\tilde{N}\tilde{P}+\tilde{H}\tilde{D})+\alpha_1\alpha_3(\tilde{H}\tilde{N}\tilde{P})+\alpha_2\alpha_4(\tilde{H}\tilde{P}\tilde{D})} + \frac{\beta_1\beta_7\tilde{D}\tilde{I} - \beta_2\beta_8\tilde{A}\tilde{N}}{1+\beta_1(\tilde{D}+\tilde{D}\tilde{I})+\beta_3(\tilde{I})+\beta_2(\tilde{N}+\tilde{A}\tilde{N})+\beta_4(\tilde{A})+\beta_1\beta_4(\tilde{D}\tilde{A})+\beta_2\beta_3(\tilde{I}\tilde{N})+\beta_1\beta_5(\tilde{D}\tilde{I}\tilde{A})+\beta_2\beta_6(\tilde{I}\tilde{A}\tilde{N})} \right) \quad 1.6$$

$$\frac{d(\tilde{D})}{d\tilde{t}} = \varepsilon_4 \left(\frac{\alpha_1\alpha_5\tilde{N}\tilde{H} - \alpha_2\alpha_6\tilde{P}\tilde{D}}{1+\alpha_1(\tilde{N}+\tilde{H}+\tilde{N}\tilde{H})+\alpha_2(\tilde{P}+\tilde{D}+\tilde{P}\tilde{D})+\alpha_1\alpha_2(\tilde{N}\tilde{P}+\tilde{H}\tilde{D})+\alpha_1\alpha_3(\tilde{H}\tilde{N}\tilde{P})+\alpha_2\alpha_4(\tilde{H}\tilde{P}\tilde{D})} - \frac{\beta_1\beta_7\tilde{D}\tilde{I} + \beta_2\beta_8\tilde{A}\tilde{N}}{1+\beta_1(\tilde{D}+\tilde{D}\tilde{I})+\beta_3(\tilde{I})+\beta_2(\tilde{N}+\tilde{A}\tilde{N})+\beta_4(\tilde{A})+\beta_1\beta_4(\tilde{D}\tilde{A})+\beta_2\beta_3(\tilde{I}\tilde{N})+\beta_1\beta_5(\tilde{D}\tilde{I}\tilde{A})+\beta_2\beta_6(\tilde{I}\tilde{A}\tilde{N})} \right) \quad 1.7$$

Where ngrid represents number of grid points the radius is split into.

At the edge of the microcompartment, I can enforce the boundary condition given by diffusive flux over the boundary:

$$\frac{d(\tilde{G})}{d\tilde{t}} = \frac{3(ngrid+{}^{1}/_{2})^{2/3} * (G_{external}-G_{boundary})\cdot\chi}{(ngrid)^{1/3}} - \frac{9(ngrid-{}^{1}/_{2})^{4/3} * (G_{boundary}-G_{MCP})\cdot\xi}{(ngrid)^{2/3}} \quad 2.1$$

$$\frac{d(\tilde{H})}{d\tilde{t}} = \frac{3(ngrid+{}^{1}/_{2})^{2/3} * (H_{external}-H_{boundary})\cdot\chi}{(ngrid)^{1/3}} - \frac{9(ngrid-{}^{1}/_{2})^{4/3} * (H_{boundary}-H_{MCP})\cdot\xi}{(ngrid)^{2/3}} \quad 2.2$$

$$\frac{d(\tilde{P})}{d\tilde{t}} = \frac{3(ngrid+{}^{1}/_{2})^{2/3} * (P_{external}-P_{boundary})\cdot\chi}{(ngrid)^{1/3}} - \frac{9(ngrid-{}^{1}/_{2})^{4/3} * (P_{boundary}-P_{MCP})\cdot\xi}{(ngrid)^{2/3}} \quad 2.3$$

$$\frac{d(\tilde{I})}{d\tilde{t}} = \frac{3(ngrid+{}^{1}/_{2})^{2/3} * (I_{external}-I_{boundary})\cdot\chi}{(ngrid)^{1/3}} - \frac{9(ngrid-{}^{1}/_{2})^{4/3} * (I_{boundary}-I_{MCP})\cdot\xi}{(ngrid)^{2/3}} \quad 2.4$$

$$\frac{d(\tilde{A})}{d\tilde{t}} = \frac{3(ngrid+{}^{1}/_{2})^{2/3} * (A_{external}-A_{boundary})\cdot\chi}{(ngrid)^{1/3}} - \frac{9(ngrid-{}^{1}/_{2})^{4/3} * (A_{boundary}-A_{MCP})\cdot\xi}{(ngrid)^{2/3}} \quad 2.5$$

$$\frac{d(\tilde{N})}{d\tilde{t}} = \frac{3(ngrid+{}^{1}/_{2})^{2/3} * (N_{external}-N_{boundary})\cdot\chi}{(ngrid)^{1/3}} - \frac{9(ngrid-{}^{1}/_{2})^{\frac{4}{3}} * (N_{boundary}-N_{MCP})\cdot\xi}{(ngrid)^{2/3}} = 0 \quad 2.6$$

$$\frac{d(\tilde{D})}{d\tilde{t}} = \frac{3(ngrid+{}^{1}/_{2})^{2/3}*(D_{external}-D_{boundary})\cdot\chi}{(ngrid)^{1/3}} - \frac{9(ngrid-{}^{1}/_{2})^{\frac{4}{3}}*(D_{boundary}-D_{MCP})\cdot\xi}{(ngrid)^{2/3}} = 0 \qquad 2.7$$

Outside the microcompartment:

$$\frac{d(\tilde{G})}{d\tilde{t}} = \frac{-3(ngrid+{}^{1}/_{2})^{2/3}*(G_{external}-G_{boundary})\cdot\chi}{(ngrid)^{1/3}} * \frac{ngrid}{Volume\ ratio} \qquad 3.1$$

$$\frac{d(\tilde{H})}{d\tilde{t}} = \frac{-3(ngrid+{}^{1}/_{2})^{2/3}*(H_{external}-H_{boundary})\cdot\chi}{(ngrid)^{1/3}} * \frac{ngrid}{Volume\ ratio} \qquad 3.2$$

$$\frac{d(\tilde{P})}{d\tilde{t}} = \frac{-3(ngrid+{}^{1}/_{2})^{2/3}*(P_{external}-P_{boundary})\cdot\chi}{(ngrid)^{1/3}} * \frac{ngrid}{Volume\ ratio} \qquad 3.3$$

$$\frac{d(\tilde{I})}{d\tilde{t}} = \frac{-3(ngrid+{}^{1}/_{2})^{2/3}*(I_{external}-I_{boundary})\cdot\chi}{(ngrid)^{1/3}} * \frac{ngrid}{Volume\ ratio} \qquad 3.4$$

$$\frac{d(\tilde{A})}{d\tilde{t}} = \frac{-3(ngrid+{}^{1}/_{2})^{2/3}*(A_{external}-A_{boundary})\cdot\chi}{(ngrid)^{1/3}} * \frac{ngrid}{Volume\ ratio} \qquad 3.5$$

$$\frac{d(\tilde{N})}{d\tilde{t}} = \frac{-3(ngrid+{}^{1}/_{2})^{2/3}*(N_{external}-N_{boundary})\cdot\chi}{(ngrid)^{1/3}} * \frac{ngrid}{Volume\ ratio} = 0 \qquad 3.6$$

$$\frac{d(\tilde{D})}{d\tilde{t}} = \frac{-3(ngrid+{}^{1}/_{2})^{2/3}*(D_{external}-G_{boundary})\cdot\chi}{(ngrid)^{1/3}} * \frac{ngrid}{Volume\ ratio} = 0 \qquad 3.7$$

Where volume ratio refers to the ratio of MCP volume to total external volume.

Initial conditions:

$$H = \frac{H_{\circ}}{{K_{M,DhaT}}^{H}} \;;\; N = \frac{N_{\circ}}{{K_{M,DhaT}}^{D}} \;;\; P = \frac{P_{\circ}}{{K_M}^{P}} \;;\; D = \frac{D_{\circ}}{{K_M}^{D}}$$

$$N = \frac{N_{\circ}}{{K_{M,IcdE}}^{N}} \;;\; D = \frac{D_{\circ}}{{K_{M,IcdE}}^{D}} \;;\; I = \frac{I_{\circ}}{{K_M}^{I}} \;;\; A = \frac{A_{\circ}}{{K_M}^{A}}$$

Results

Once appropriate parameters were defined, all equations were integrated over time. Nondimensional parameter estimates used to conduct a sensitivity analysis of total flux are shown in Table 1. From sensitivity analysis, it was evident that particular parameters caused significant overall change while others did not. High sensitivity was observed to changes in alpha5, beta7, and epsilon1 parameters (Figures 2) when compared to the initial condition (Figure 3).

Table 1. Nondimensional parameter estimates used for sensitivity analysis

Parameter	Meaning	Estimated Value
α_1	${K_{M,DhaT}}^{N}/{K_{I,DhaT}}^{N}$	0.001
α_2	${K_{M,DhaT}}^{D}/{K_{I,DhaT}}^{D}$	0.001
α_3	${K_M}^{P}/{K_I}^{P}$	0.001
α_4	${K_M}^{H}/{K_I}^{H}$	0.001
α_5	${V_{f,DhaT}}^{max}/V_{DhaB}$	0.5
α_6	${V_{r,DhaT}}^{max}/V_{DhaB}$	0.1
β_1	${K_{M,DhaT}}^{D}/{K_{I,IcdE}}^{D}$	0.0023
β_2	${K_{M,DhaT}}^{N}/{K_{I,IcdE}}^{N}$	0.0004
β_3	${K_{M,IcdE}}^{D}/{K_{I,IcdE}}^{D}$	0.001
β_4	${K_{M,IcdE}}^{N}/{K_{I,IcdE}}^{N}$	0.001
β_5	${K_M}^{A}/{K_I}^{A}$	0.001
β_6	${K_M}^{I}/{K_I}^{I}$	0.001
β_7	${V_{f,IcdE}}^{max}/V_{DhaB}$	0.5
β_8	${V_{r,IcdE}}^{max}/V_{DhaB}$	0.1
ε_1	$K_{M,DhaB}/{K_{M,DhaT}}^{H}$	15
ε_2	$K_{M,DhaB}/{K_{M,DhaT}}^{P}$	0.12
ε_3	$K_{M,DhaB}/{K_{M,DhaT}}^{N}$	9.09
ε_4	$K_{M,DhaB}/{K_{M,DhaT}}^{D}$	3.91
ε_5	$K_{M,DhaB}/{K_{M,DhaT}}^{A}$	0.12
ε_6	$K_{M,DhaB}/{K_{M,DhaT}}^{I}$	1.5

Figure 2. Sensitivity Analysis of pathway with respect to parameters. Plotted is fold change of max 3-HPA intermediate after perturbation as compared to initial conditions. **(A)** Orange bars indicate change upon a 10% decrease in the indicated parameter; blue bars indicate the change upon a 10% increase in the indicated parameter. **(B)** 10% increase in indicated parameters **(C)** 10% decrease in indicated parameter.

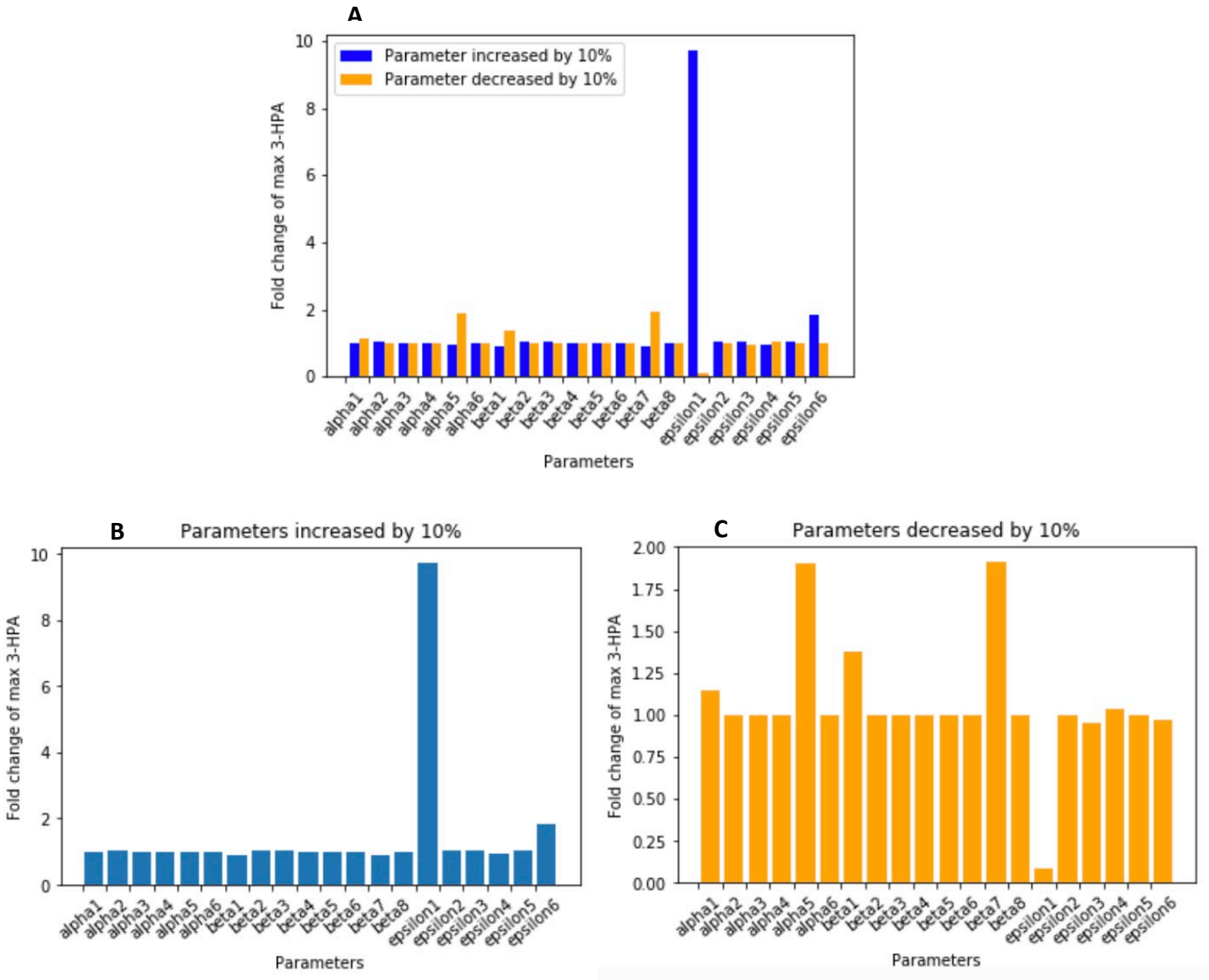

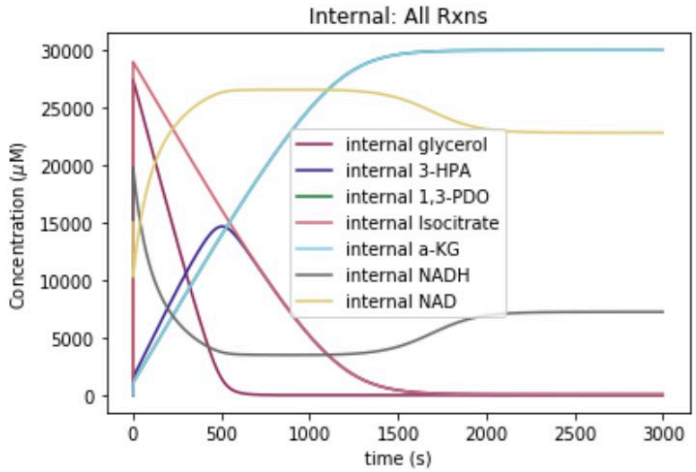

Figure 3. Integration over time using initial conditions

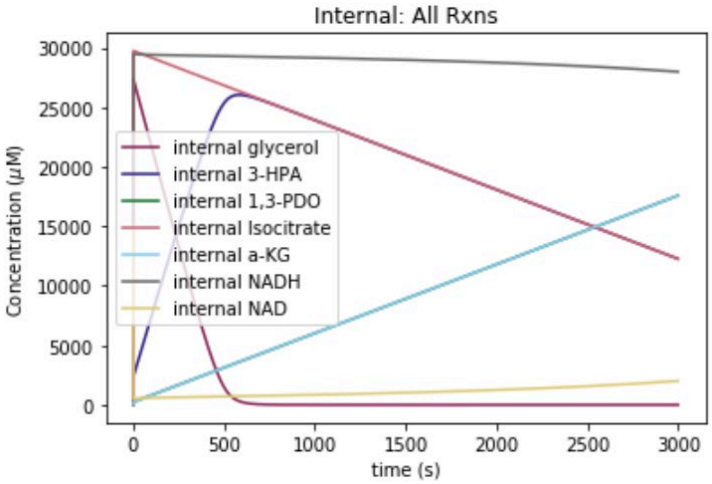

Figure 4. Integration over time with 10 fold decrease of alpha 5

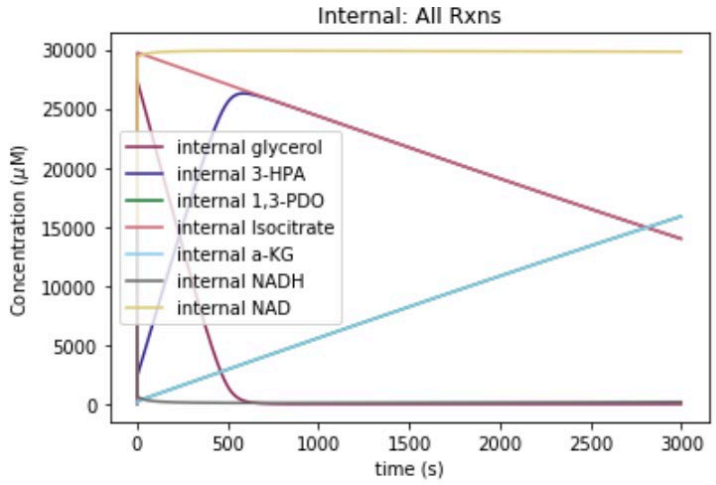

Figure 5. Integration over time with 10 fold decrease in beta 7

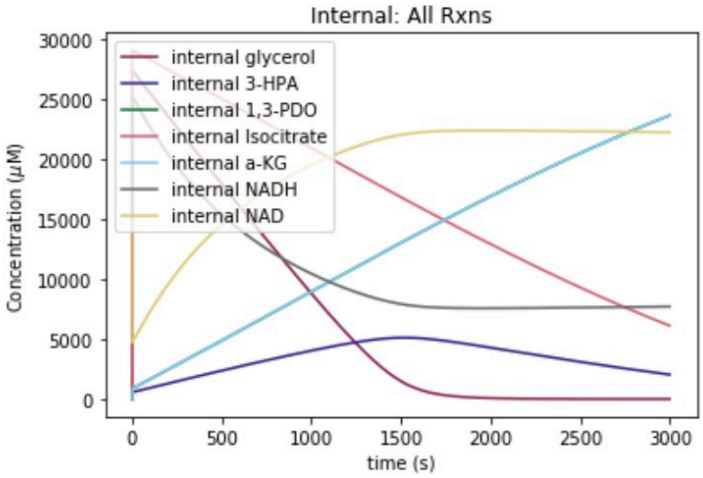

Figure 6. Integration over time with 5 fold decrease of epsilon 1

References

[1] Jakobson, C.M., Tullman-Ercek, D., Slininger, M.F., and Mangan, N.M. (2017). A systems-level model reveals that 1,2-Propanediol utilization microcompartments enhance pathway flux through intermediate sequestration. PLoS Comput. Biol. 13(5).

[2] Tong, I.T., Liao, H.H., Camer, D.C. (1991). 1,3-Propanediol production by Escherichia coli expressing genes from the Klebsiella pneumoniae dha regulon. Appl. Environ. Microbiol. 57(12),3541-3546

[3] Celinska, E. (2010). Debottlenecking the 1,3-propanediol pathway by metabolic engineering. Biotechnol. Adv. 28(4), 519-530.